https://doi.org/10.30799/jnst.253.19050412 J. Nanosci. Tech. - Volume 5 Issue 4 (2019) 787–790

ISSN: 2455-0191

Share Your Innovations through JACS Directory

Journal of Nanoscience and Technology

Visit Journal at http://www.jacsdirectory.com/jnst

Effect of Temperature on Different Properties of ZnS Nanoparticles Synthesized by Solid-State Reaction Method

S. Suganya, M. Jothibas*, A. Muthuvel

PG & Research Department of Physics, TBML College, Porayar – 609 307, Tamilnadu, India.

ARTICLEDETAILS

Article history:
Received 16 May 2019
Accepted 01 June 2019
Available online 12 June 2019

Keywords:
ZnS NPs
Solid-State Study
Optical Properties

ABSTRACT

We report that results of investigation of the ZnS nanoparticles were synthesized by solid state reaction method at different annealing temperature (350 °C, 400 °C and 450 °C). The structural, functional, morphological and optical properties were characterized by using X-ray diffraction (XRD) analysis, Fourier transform infrared (FTIR) spectroscopy, UV-Vis spectroscopy, photoluminescence (PL) spectroscopy and scanning electron microscopy (SEM) with energy dispersive X-ray analysis. XRD patterns confirmed to the ZnS nanoparticles have cubic crystal structure and crystalline nature. The FTIR spectroscopy shows the bonding nature and presence the metal oxide nanoparticles. The blue shift absorption was observed from the UV-visible spectrum. The photoluminescence spectra showed a two emission peaks corresponding to blue-green emission. A SEM photograph shows the spherical shaped nanoparticles and the elements Zn and S alone are identified from EDS.

1. Introduction

Nanotechnology refers to any technology in nanoscale that contains applications in the real world, it combines the production and use of physical and biological systems into individual systems or molecules from the submicron dimension, as well as the integration of the resulting nanostructures into larger systems. Semiconductor nanocrystals have been studied extensively by scientists due to the most effective applications in recent years. Among these ZnS semiconductor compound is considered to be one of the most outstanding functional materials owing to its non-toxicity [1] high thermal stability, high transparency [2] ability of developing optoelectronic application including electroluminescent devices, light emitting diodes, lasers, sensors, flat panel displays [3]. ZnS nanoparticles could be used as good catalysts due to rapid generation of the electron-hole pairs by photo-excitation and highly negative reduction potentials of excited electrons as conduction band position of ZnS in aqueous solution in higher than that of other semiconductors such as TiO_2 and ZnO [4] A large surface ratio of the surface of an catalyst helps the best catalytic activity [5,6]. The size of large-scale surface area. The higher surface area of the surface causes the rise of the surface states, which will change the function of the electrons and the holes, chemical reaction affects the mechanism. photocatalysts found many applications in the environment agueous solution [7]. Air purification, metal recovery, and especially recently, produce self-cleaning glass surface [8]. Applications for removal of water reactor have been piloted. Motions are the source of artificial radiation in the market. Many techniques are used to integrate ZnS nanoparticles chemical vapor deposition [9], wet chemical route [10], gas phase condensation method [11], co-precipitation method [12], solvothermal synthesis [13], hydrothermal process [14] thermal decomposition method [15] radio frequency magnetron sputtering technique [16] and solid state reaction method are used to consolidate ZnS nanopaticles, synthesized at different calcination temperatures (350 °C, 400 °C and 450 °C.).

2. Experimental Methods

In this study, zinc acetate dihydrate and thiourea were used to form ZnS nanoparticles by solid state reaction method. These chemicals were directly used without special treatment. For typical synthesis, zinc acetate dihydrate and thiourea were ground separately using agate mortar. Then appropriate amount of these precursors was mixed together and ground thoroughly. Finally, mixed powder was heated in a muffle furnace for 4 h at 350 °C, 400 °C and 450 °C respectively (Fig. 1). Wang and Hong adopted these methods to prepare ZnS nanoparticles [17].

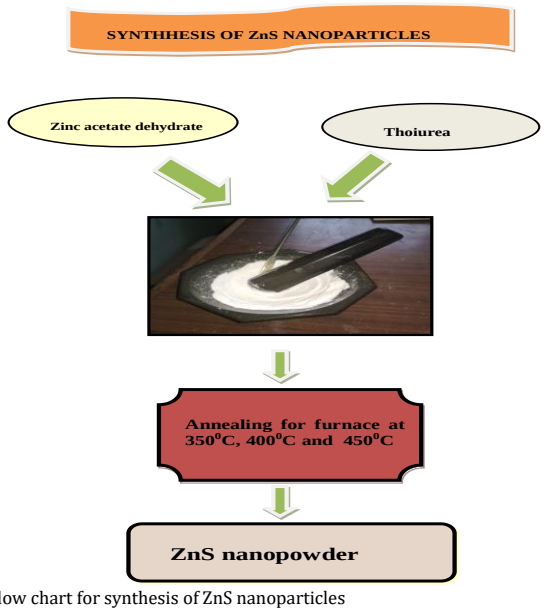

Fig. 1 Flow chart for synthesis of ZnS nanoparticles

The crystal structure of ZnS nanoparticles was examined by X-ray diffraction analysis using SHIMADZU 6000 X-ray diffractometer with Cukα radiation at room temperature. The chemical structure was investigated by SHMADZU. Optical absorption spectra were recorded in the range 200-1200 nm using JASCO v-670 spectrometer. The photoluminescence (PL) behaviour was studied at room temperature by Plorolog 3-HORIBA JOBIN YUON with an excitation wavelength of 325 nm. The surface morphology and elemental composition of the product was demonstrated by SEM with EDX analysis using JEOL JSM 6390.

*Corresponding Author:jothibas1980@gmail.com(M. Jothibas)

https://doi.org/10.30799/jnst.253.19050412

Cite this Article as: S. Suganya, M. Jothibas, A. Muthuvel, Effect of temperature on different properties of ZnS nanoparticles synthesized by solid-state reaction method, J. Nanosci. Tech. 5(4) (2019) 787–790.

3. Results and Discussion

3.1 XRD Analysis

The XRD patterns of ZnS nanoparticles synthesized at various temperature (350 °C, 400 °C and 450 °C) using solid state reaction method in Fig. 2. Three strong peaks are observed at 2θ values of 28.360°, 47.883° and 56.350° corresponding those from (111), (220) and (311) planes in all samples belonging to a cubic phase of ZnS nanoparticles. These plans are matched with standard JCPDS card no (05-0566) and it reported that [18] no impurity peaks are appearing in this sample. The strong prominent peak of the plane (111) to compare with the low intensity reflections (220) and (311) planes [19].

The broadening of the peaks indicates the nanocrystalline nature of the sample. The average crystalline size is 2θ and the full width half maximum (hkl) peaks using Debye-Scherrer's relation. The average crystal size is 3.71, 3.68 and 3.76 nm. Crystal size was decreased; thus, we can say that size of nanoparticles decreases when calcination temperature has increases upto 400 °C. The growth of crystal is improved and imperfections or defects in crystal decrease. At higher temperature (450 °C) perhaps, the reaction gets more energy to grow with larger grain size. This indicates can be adjusted by controlling the temperature of the reaction. Thus, the dislocation is an imperfection in a crystal associated with misallocated of the lattice in one part to another part. Dislocation density (δ) is defined as the length of dislocation lines per unit volume of the crystal and was evaluated by using the relation, $\delta=1/D^2$, where, D is the crystallite size obtained from XRD data. The dislocation density has decreases upto 400 °C. The dislocation density has decreases with decreasing crystal size. At higher temperature, perhaps the dislocation density has increases.

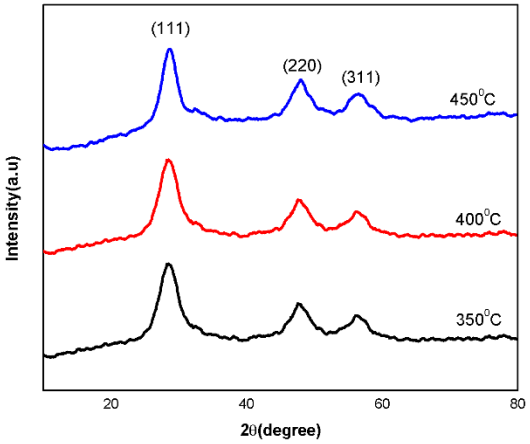

Fig. 2 XRD patterns of ZnS nanoparticles

Table 1 2θ values corresponding to peaks, d-spacing of the planes, crystal size, average crystal size of ZnS nanoparticles

Sample at °C	2θ degree	plane	d space	FWHM	Cosθ	Crystal size D (nm)	Average crystal size(nm)
	28.6300	111	3.1154	3.1600	0.96	3.4026	
350	47.8833	220	1.8982	3.2667	0.91	3.7688	3.71
	56.3500	311	1.6314	3.5000	0.88	3.9854	
	28.3166	111	3.1492	2.7330	0.96	3.1897	
400	47.5375	220	1.9112	2.6750	0.91	3.3879	3.68
	56.4125	311	1.6300	2.1000	0.88	4.4714	
	28.4150	111	3.1385	2.8700	0.96	2.9810	
450	47.5604	220	1.9103	2.0458	0.91	4.4303	3.76
	56.2375	311	1.6344	2.4250	0.88	3.8792	

Table 2 Dislocation density, microstrain, lattice constant of ZnS nanoparticles

Sample at °C	Dislocation density δ	Microstrain ε(10^{-3})	Lattice constant Å	Average lattice constant
	9.1416	0.0135	5.4042	
350	5.2243	0.0130	5.3892	5.3994
	4.2842	0.0134	5.4049	
	9.7796	0.1132	5.4545	
400	8.7122	0.0106	5.4056	5.4221
	4.9197	0.0080	5.4063	
	11.253	0.0121	5.4360	
450	5.0948	0.0081	5.4032	5.4197
	6.0477	0.0093	5.4200	

The microstrain εhkl in the synthesized sample was calculated by using the relation [20]. The microstrain value has decreases up to $0.0135x10^{-3}$ to $0.0121x10^{-3}$.

$$\varepsilon = \frac{\beta\cos\theta}{4}$$

The lattice parameters a,b,c for the cubic structure can be determined by the following equation,[21].

$$d = \frac{a}{\sqrt{h^2 + k^2 + l^2}}$$

where h, k and l are the miller indices of the peak. The structural parameters are shown in Tables 1 and 2.

3.2 FTIR Spectral Studies

The FTIR spectrum of the ZnS nanoparticles in the frequency range of 400-4000 cm^{-1} reveals the various vibrations involved in the molecules. Fig. 3 shows the FTIR peaks of ZnS nanoparticles at different temperature. This spectrum clearly shows the functional groups. Several peaks are observed at 3257, 2355, 2181, 2060, 1393, 1116, 798 and 614 cm^{-1} for the pure ZnS shows in Table 3. The broad absorption peaks at 3257 cm^{-1} are attributed at O-H stretching. 2355, 2181, and 2060 cm^{-1} are due to C=O stretching. The peaks appearing at 798 and 614 cm^{-1} are attributed to Zn-S vibration and are characteristic of cubic ZnS.

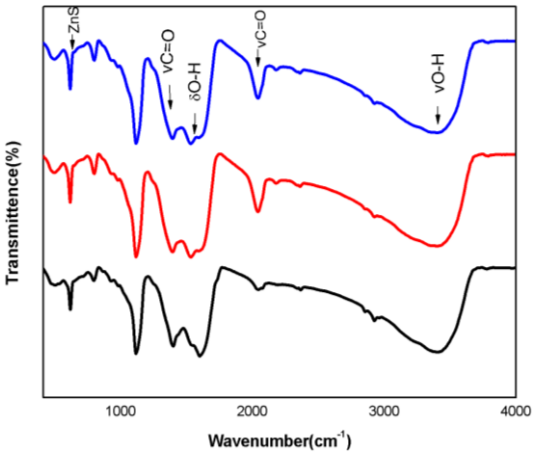

Fig. 3 FTIR spectra of ZnS nanoparticles

Table 3 Tentative vibration in the ZnS nanoparticles

Vibrational assignments	Experimental absorption (cm^{-1})
O-H stretching	3257
C-H stretching	2355
Co_2 molecules	2181, 2060
O-H bending	1393
Carboxyl and methylene groups	1116
Zn-S stretching	798
Cubic ZnS	614

3.3 UV–Visible Spectroscopy

UV-visible spectroscopy refers to the absorption or reflectance spectroscopy in the ultraviolet visible spectral region. This means it uses light in the visible is adjacent ranges. The absorption or reflectance in the visible range directly affects the perceived color of the chemicals involved. In the region of the electromagnetic spectrum atoms and molecules undergo electronic transitions. Absorption spectroscopy is complementary to fluorescence spectroscopy in that fluorescence deals with transitions from excited state to the ground state while absorption measures transition from the ground state to the excited state [22]. The absorption spectra of the prepared ZnS nanoparticles were illustrated in Fig. 4. The absorption co-efficient is calculated using the formula,

$$\alpha = \frac{2.303A}{l}$$

where, A is the absorbance and l is the path length. The value of optical band gap is determined from the absorption spectra using the Tauc relation,

$$\alpha h\gamma = A(h\gamma - Eg)^n$$

https://doi.org/10.30799/jnst.253.19050412

Fig. 5 shows the curves of $(\alpha h\gamma)^2$ versus hν for ZnS nanoparticles prepared at different temperatures. The Eg values are obtained by extrapolating the straight-line portions of the graph to the X-axis. The measured energy bandgaps from these plots are represented in Table 4. From these table, it can be obsrerved that the Eg values varied from 3.54 to 3.66 eV for ZnS nanoparticles at different temperature. The 400 °C for exhibiting higher bandgap energy 3.66 eV. So it ha been taken as optimum compound for further investigation.

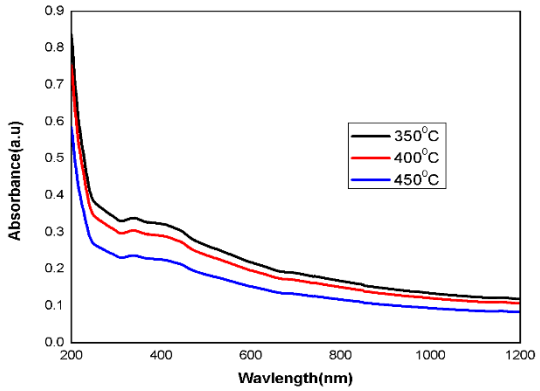

Fig. 4 Optical spectra of ZnS nanoparticles

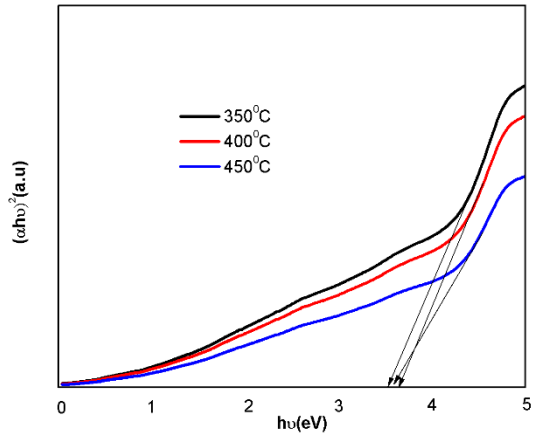

Fig. 5 Plot of $(\alpha h\gamma)^2$ versus hγ for ZnS nanoparticles

Table 4 Bandgap energy for ZnS nanoparticles

ZnS	Bandgap energy(eV)
350⁰C	3.54
400⁰C	3.66
450⁰C	3.59

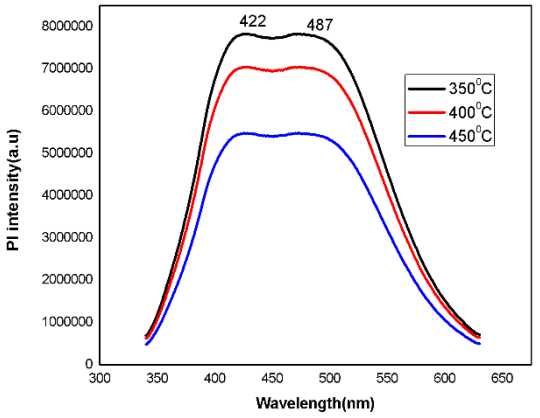

Fig. 6 Photoluminescence study for ZnS nanoparticles at different temperature

3.4 Photoluminescent Spectroscopy

Photoluminescence is a vital tool to explore the quantity of nanoparticles which depends on the size of the crystallites, morphology and chemical environment. PL is a process in which a molecule absorbs a photon in the visible region, exciting one of its electrons to a higher electronic excited state, and then radiates a photon as the electrons returns to a lower energy state. PL spectra of ZnS nanoparticles among different temperatures (350 °C, 400 °C and 450 °C) at excitation wavelength is around 325 nm as shown in Fig. 6. The peak observed in the 422-487 nm may be attributed to the near band emission. It is well reported that Schotty defects pin cubic Zn [23,24] depict emission peak around 425 nm in ZnS nanoparticles due to sulfur vacancies [25] also represented peak around 422 nm credited to sulfur vacancies. [26] reported emission range is 431-438 nm attributed sulfur vacancies i.e.due to recombination of electrons at the sulfur vacancies [27]. Reported the 420-487 nm may be attributed sulfur vacancies i.e due to recombination of electrons at the sulfur vacancies with holes in the valence band. Based on these our work, the range of the ZnS nanoparticles 422 nm (blue) may be assign to the composition of the electrons from the conduction band and holes from the valence band. The emission peak at 487 nm can be connected with sulfur vacancy.

3.5 Morphological Characterization

Scanning electron microscope is a type of electron microscope that produces images of a sample by scanning the surface with a focused beam of electrons. nanoparticle analysis using a SEM supplemented by EDX was carried out for the cubic ZnS to establish the morphology, grain size, shape and to confirm their chemical composition SEM observed the nano-sized ZnS grains as large surface area with well-defined mesopores and the images are shown in Fig. 7(a-c) at different magnification. These micrographs confirm that the grown in a very high intensity. Besides the uniform distribution of distribution of particles was found and they consist of either some single particle or a cluster of particles. A closer examination of these pictures reveals a well-defined particle-like morphology having abudence of spherical shaped particles. The EDX analysis Fig. 7(d) clearly showed clearly showed that the presence of elements such as Zn and Sulfide only. The strong X-ray peaks associated with Zn and S. Atomic is weight percentage are shown in Table 5.

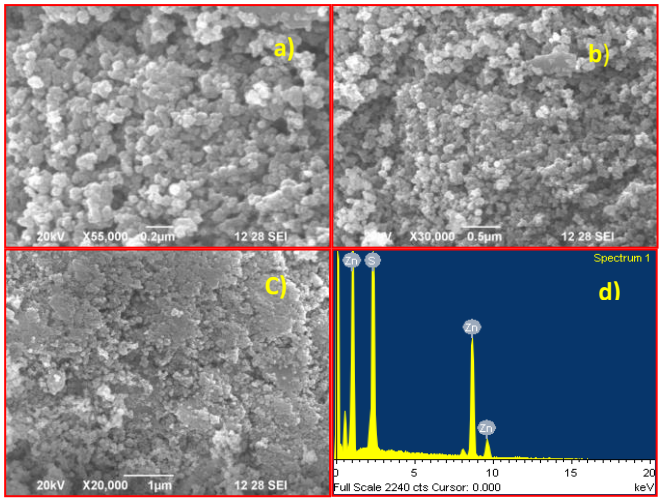

Fig. 7 SEM and EDX analysis of ZnS nanoparticles

Table 5 The EDS analysis of ZnS nanoparticles

Element	Atomic percentage (at.%)	Weight percentage (wt.%)
Zn	24.91	40.34
S	75.09	59.66
Total	100	100

4. Conclusion

The ZnS nanoparticles with different sintering temperatures have been successfully synthesized by solid-state reaction method. The XRD results reveal that the particles are crystalline nature and cubic crystal structure with strong preferred orientation along (111) plane. The blue shift absorption in UV-visible region. Optical band gap energy has 3.6 eV. The PL studies showed the existence of sulphur and zinc vacancies in ZnS nanoparticles. The SEM photographs showed spherical shape morphology.

References

[1] A. Le Donne, S. Kanti Jana, S. Banerjee, S. Basu, S. Binetti, Optimized luminescence properties of Mn doped ZnS nanoparticles for photovoltaic applications, J. Appl. Phys. 113 (2013) 014903:1-5.

[2] K. Nagamani, N. Revathi, P. Prathap, Y. Lingappa, K.T.R. Reddy, Al-doped ZnS layers synthesized by solution growth method, Curr. Appl. Phys. 12 (2012) 380–384.

https://doi.org/10.30799/jnst.253.19050412

[3] X. Fang, T. Zhai, U.K. Gautam, L. Li, L. Wu, Y. Bando, ZnS nanostructures: From synthesis to applications, Prog. Mater. Sci. 56 (2011) 175–287.
[4] J.Y. Liao, K.C. Ho, A photovoltaic cell incorporating a dye-sensitized ZnS/ZnO composite thin film and a hole-injecting PEDOT layer, Sol. Energy Mater. Sol. Cells. 86 (2005) 229-241.
[5] Li, X.Y. He, M.H. Cao, Micro-emulsion-assisted synthesis of ZnS nanospheres and their photocatalytic activity, Mater. Res. Bull. 43 (2008) 3100-3110.
[6] H.F. Shi, X.K. Li, D.F. Wang, Y.P. Yuan, Z.G. Zou, J.H. Ye, Photoreduction of carbon dioxide over $NaNbO_3$ nanostructured photocatalysts, Catal. Lett. 141(4) (2011) 525-530.
[7] R.W. Matthews, E. Pelizzetti, M. Schiavello, Proceedings of the Eighth International Conference on Photochemical Conversion and Storage of Solar Energy, IPS-8, Palermo, Italy, 1991, pp.15-20.
[8] P. Pichat, J. Disdier, C. Hoang-Van, D. Mas, G. Goutailler, C. Gaysse, Purification/deodorization of indoor air and gaseous effluents by TiO_2 photocatalysis, Catal. Today 63 (2000) 363-369.
[9] A.K. Kole, S.Gupta, P. Kumphakar, P.C. Ramamurthy, Nonlinear optical second harmonic generation in ZnS quantum dots and observation on optical properties of ZnS /PMMA nanocomposites, Optics Commun. 313 (2014) 231-237.
[10] M. Navaneethan, J. Archana, K.D. Nisha, Y. Hayakawa, S. Ponnusamy, C. Muthamizhchelvan, Temperature dependence of morphology, structural and optical properties of ZnS nanostructures synthesized by wet chemical rout, J. Alloys Compd. 506 (2010) 249-252.
[11] J.C. Sanchez-Lopez, A. Fernandez, The gas-phase condensation method for the preparation of quantum-sized ZnS nanoparticles, Thin Solid Films 317 (1998) 497-499.
[12] Hassan Ali, S. Karim, M.A. Rafiq, K. Maaz, Atta Ur Rahman, A. Nisar, M. Ahmad, Eletrical conduction mechanism in ZnS nanoparticles, J. Alloy. Compd. 612 (2014) 64-68.
[13] L. Dong, Y. Chu, Y. Zhang, Microemulsion-medicated solvothermal synthesis of ZnS nanowires, Matt. Lett. 61 (2007) 4651-4654.
[14] J. Zhao, R. Liu, Surfactant–free hydrothermal synthesis and optical properties of ZnS solid microspheres, Mater. Lett. 124 (2014) 239-241.
[15] P.K. Ghosh, U.N. Maiti, S. Jana, K.K. Chattopadhyay, Field emission from ZnS nanorods synthesized by radio frequency magnetron sputtering technique, Appl. Surf. Sci. 253 (2006) 1544-1550.
[16] W. Zhang, Xianghua Zeng, Hongetei Liu, Junfeng Lu, Synthesis and investigation of blue and green emission of ZnS ceramics, Lumin. 134 (2013) 498-503.
[17] L.P. Wang, G.Y. Hong, A new preparation of zinc sulfide nanoparticles by solid state method at low temperature, Mater. Res. Bull. 35 (2000) 695-701.
[18] M. Mubashshir, H. Farooqi, Rajneesh K. Srivastava, Structural, optical and photoconductivity study of ZnS nanoparticles synthesized by a low temperature solid state reaction method, Mater. Sci. Semicond. Proces. 20 (2014) 61-67
[19] M. Jothibas, S. Johnson Jeyakumar, C. Manoharan, I. Kartharinal Punithavathy, P. Praveen, J. Prince Richard, Structural and optical properties of zinc sulphide nanoparticles synthesized via solid state reaction method, J. Mater. Sci. 28 (2016) 1889-1894.
[20] G. Murugadoss, M. Rajesh Kumar, Synthesis and optical properties of monodispersed Ni^{2+} doped ZnS nanoparticles, Appl. Nanosci. 4 (2014) 67-75.
[21] R. Sathish Kumar, S. Johnson Jeyakumar, M. Jothibas, I. Kartharinal Punithavathy, J. Prince Richard, Influence of molar concentration on structural, optical and magnetic properties of NiO nanoparticles, J. Mater. Sci. 28(20) (2017) 15668-15675.
[22] Douglas A. Skoong, Stanley R Ctouch, E. James Holitor, Instrumental Analysis, 6th Edn., Thomson Books, Canada, 2007.
[23] S.S. Kumar, M.A. Khadar, S.K. Dhara, T.K. Ravindran, K.G.M. Nair, Photoluminescence and Raman studies of ZnS nanoparticles implanted with Cu^+ ions, Nucl. Instrum. Meth. B 251 (2004) 435-440.
[24] P.H. Borse, N. Deshmukh, R.F. Shinde, S.K. Date, S.K. Kulkarni, Luminescence quenching in ZnS nanoparticles due to Fe and Ni doping, J. Mater. Sci. 34 (1999) 6087-6089.
[25] H.Y. Lu, S.Y. Chu, S.S. Tan, The characteristics of low-temperature-synthesized ZnS and ZnO nanoparticles, J. Cryst. Growth 269 (2004) 385-381.
[26] Palvinder Kaur, Sanjeev Kumar, Chi-Liang Chen, Kai-Siang Yang, Da-Hua Wei, et al., Gd doping induced weak ferromagnetic ordering in ZnS nanoparticles synthesized by low temperature co-precipitation technique, Mater. Chem. Phys. 186 (2016) 124-130.
[27] G.S. Lotey, Z. Jindal, V. Singhi, N.K. Verma, Structural and photoluminescence properties of Eu doped ZnS nanoparticles, Mater. Sci. Semicond. Proces. 16 (2013) 2044-2050.

https://doi.org/10.30799/jnst.253.19050412

Cite this Article as: S. Suganya, M. Jothibas, A. Muthuvel, Effect of temperature on different properties of ZnS nanoparticles synthesized by solid-state reaction method, J. Nanosci. Tech. 5(4) (2019) 787–790.